

See discussions, stats, and author profiles for this publication at: <https://www.researchgate.net/publication/241277322>

Coal Swelling Model for High Heating Rate Pyrolysis Applications

ARTICLE *in* ENERGY & FUELS · APRIL 2011

Impact Factor: 2.79 · DOI: 10.1021/ef200240u

CITATIONS

16

READS

51

3 AUTHORS, INCLUDING:



Kolbein K. Kolste

Dartmouth College

14 PUBLICATIONS 34 CITATIONS

SEE PROFILE



Thomas H. Fletcher

Brigham Young University - Provo Main Cam...

155 PUBLICATIONS 2,299 CITATIONS

SEE PROFILE

Coal Swelling Model for High Heating Rate Pyrolysis Applications

Randy C. Shurtz, Kolbein K. Kolste, and Thomas H. Fletcher*

Department of Chemical Engineering, Brigham Young University, Provo, Utah 84602, United States

ABSTRACT: Thermal swelling of coal during pyrolysis strongly influences combustion and gasification rates. Coal swelling is known to vary strongly with coal rank, heating rate, and total pressure. New experiments confirm and clarify previous observations that maximum swelling occurs for high-rank bituminous coals at heating rates slightly below 10^4 K/s. Advanced swelling models based on bubble physics yield good qualitative trends at low heating rates, but they fail to predict observed decreases in coal swelling as particle heating rates increase beyond 10^4 K/s. An empirical swelling correlation for computational fluid dynamics (CFD) applications that correctly describes experimentally observed trends with the heating rate is proposed. Model parameters were fit to data from the literature using a coal rank index based on the chemical structure of the coal. The correlation has a form that allows for calculation of shrinkage for lignites, increasing swelling ratios as rank increases from sub-bituminous to bituminous ranks, and decreasing swelling ratios as rank increases from low volatile bituminous to anthracite. The correlation accurately predicts swelling as a function of coal rank and heating rate at atmospheric pressure.

1. INTRODUCTION

Changes in the structure of a coal particle during pyrolysis influence the subsequent reaction history in various ways. The magnitude and accessibility of the surface area for heterogeneous reaction on the interior surfaces of the char particles determine the reaction rate at a given temperature. The temperatures at which different physical processes dominate the observed reaction rate have been described in terms of three zones.¹ At low temperatures (zone I), oxidation or gasification kinetics are rate-limiting, while diffusion of reactants through the particle boundary layer is rate-limiting at very high temperatures (zone III). At intermediate temperatures (zone II), both reaction kinetics and diffusion through pores determine the observed reaction rates. Practical applications of combustion and gasification of pulverized coal typically occur in zone II, where the particle size and pore structure strongly influence the rates at which gaseous reactants are transported to the internal surfaces of the char.

Descriptions of char structure include various measures of surface area, pore structure, and internal voids caused by bubble growth. Detailed systems have been developed for the classification of char based on morphological characteristics, which are beginning to come into use in advanced combustion and gasification models.² However, the swelling ratio d/d_0 is the most common parameter used to describe char structure in combustion modeling. It is likely to remain the preferred method because of its simplicity. For highly swollen cenospheres, the particle wall thickness is very small compared to the particle diameter; the volume of the internal void may be only slightly less than the total volume of the particle. In such cases, knowledge of the particle size is critical for accurate models of transport processes and, hence, reaction rates. Knowledge of the particle size and the pyrolysis yield can be used to estimate the wall thickness for cenospheres, which is another critical parameter for calculating transport rates.

Thermal swelling of coal varies strongly with coal rank, heating rate, and total pressure.^{3,4} Maximum temperature and initial particle size influence swelling mainly through their effect on the

heating rate. Particles of approximately $50\ \mu\text{m}$ mean diameter are typically used in pulverized coal boilers and gasifiers, with particle heating rates of about 10^6 K/s and maximum temperatures that may exceed $2000\ ^\circ\text{C}$. At conditions found in pulverized coal boilers and gasifiers, the effect of ambient gas composition on swelling is probably small because the blowing effect inhibits transport of surrounding gases to the surface of pyrolyzing coal particles. Maximum swelling occurs for high-rank bituminous coals at heating rates slightly below 10^4 K/s (Figure 1).⁵ Bituminous coal swelling ratios can decrease from greater than 1.5 to less than 1.05 as heating rates increase beyond 10^4 K/s at atmospheric pressure. Therefore, swelling measurements at heating rates lower than 10^5 K/s may only be appropriate for the largest particles of the distributions used in industrial pulverized coal boilers and gasifiers.

Swelling behavior can be conveniently viewed in terms of two regimes of heating rate (Figure 1). Electrically heated reactors with stationary particles (thermogravimetric analyzers and wire-mesh reactors) usually operate at heating rates below 10^3 K/s in regime 1. Electrically heated entrained-flow reactors (e.g., drop-tube furnaces) typically operate near 10^4 K/s, which is slightly above the lower boundary of regime 2. Flat-flame burners typically operate closer to 10^5 K/s for particles smaller than $\sim 100\ \mu\text{m}$. The details of swelling behavior at the transition between these two regimes is very difficult to characterize experimentally because of equipment limitations and uncertainties in the calculated particle heating rate.

The most advanced swelling models are based on the physics of bubble formation in the metaplast or coal melt during pyrolysis.⁸ Tools of this type are excellent resources for investigating swelling from a theoretical point of view. However, they have several practical limitations. First, input parameters can be difficult to obtain. It is practically impossible to measure physical properties, such as viscosity, in reacting metaplast, and other detailed inputs,

Received: February 15, 2011

Revised: April 1, 2011

Published: April 11, 2011

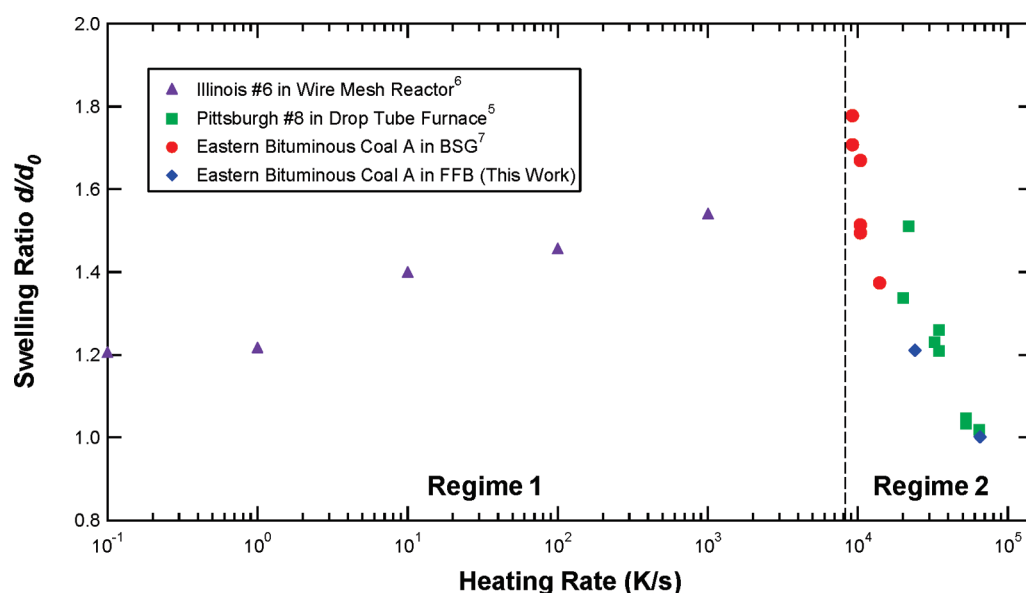


Figure 1. Atmospheric swelling as a function of the heating rate, denoting regimes of increasing/decreasing swelling.^{5–7}

Table 1. Characteristics of Eastern Bituminous Coal A Used in This Study

particle size (μm)	149–177	88–105	53–66
C (% daf)	79.08	78.68	79.00
H (% daf)	5.84	5.79	5.73
N (% daf)	1.49	1.51	1.53
S + O (% daf, by difference)	13.59	14.02	13.74
volatile matter (% daf)	47.87	46.98	48.75
ash (% dry)	7.36	6.88	6.90
moisture (% as received)	4.65	5.1	4.43

such as density distributions, are inconvenient to measure. Second, the computational burden for each particle is too high for most computational fluid dynamics (CFD) applications. Third, existing bubble models do not predict the decrease in swelling that has been observed as heating rates increase from 10^4 to 10^5 K/s (Figure 1).⁹ Most empirical swelling models also fail to predict decreased swelling in regime 2 because they lack heating rate dependence of any kind.^{10,11} This decrease in swelling has been attributed to a high rate of devolatilization that is faster than the relaxation time of the viscous coal melt.⁵ The bubbles burst at very high heating rates, followed by cross-linking.

The ability to make improved estimates of the swelling ratio at industrial conditions is of great practical interest in combustion and gasification modeling. In this study, new swelling data are presented that illustrate the effect of heating rate. Also, a new coal-dependent swelling correlation with heating rate dependence is developed for use at atmospheric pressure. Methods to extend this model to elevated pressures are under development and will be treated in future publications.¹² The performance of the new swelling correlation is evaluated through comparisons to published experimental data as well as recently acquired data.

2. EXPERIMENTAL SECTION

A U.S. coal designated as “eastern bituminous coal A” was studied at atmospheric pressure as a function of heating rate (Table 1). The

Table 2. Experimental Conditions for Eastern Bituminous Coal A at 0.84 atm

particle size (μm)	149–177	88–105	53–66
swelling ratio, d/d_0 (ash tracer)	1.21	1.00	0.93
density ratio, ρ/ρ_0 (tap technique)	0.24	0.39	0.51
volatiles yield (% daf, ash tracer)	61.2	63.4	61.4
volatiles yield (% daf, average of Si and Al)	69.4	67.7	N/A
heating rate (K/s)	2.4×10^4	6.5×10^4	1.5×10^5
collection height (in.)	6	3.5	2
residence time (ms)	90	48	25

Brigham Young University (BYU) atmospheric flat-flame burner (FFB) used in this study has been described previously.^{13,14} Heating rates near 10^5 K/s are typical for this facility, and the local ambient pressure is 0.84 atm. Experiments with three different particle sizes were conducted to vary the heating rate. A fuel-rich CO flame with a peak centerline gas temperature of 1546 K was used for these experiments.¹² Residence times corresponding to full pyrolysis were chosen based on calculations using the CPD model.^{15,16}

In collaboration with this work, pyrolysis experiments were performed elsewhere on the same coal. The other experiments were conducted in a bench-scale gasifier (BSG), which is similar to an atmospheric drop-tube reactor (Figure 1).⁷ The heating rate of the BSG can exceed 10^4 K/s at temperatures of up to 1400 °C at atmospheric pressure. The BSG provides particle residence times of up to 2–3 s. The BSG has a gas-quenched collection probe with an aerodynamic separation system for separating char from soot that is similar in design to the BYU FFB.

The experiments were performed using two facilities to investigate a greater range of heating rates than would be possible with a single facility. The BSG achieved heating rates between 9.2×10^3 and 1.4×10^4 K/s; the highest heating rates were attained by adding oxygen to the gas stream to burn some of the volatiles. The FFB was chosen to complement the BSG experiments because the heating rates from 2.4×10^4 to 1.5×10^5 K/s in the FFB are closer to those found in utility boilers and gasifiers.

The experimental volatiles yield determined from samples collected in the BYU FFB using an ash tracer technique was 61–63 wt % dry and

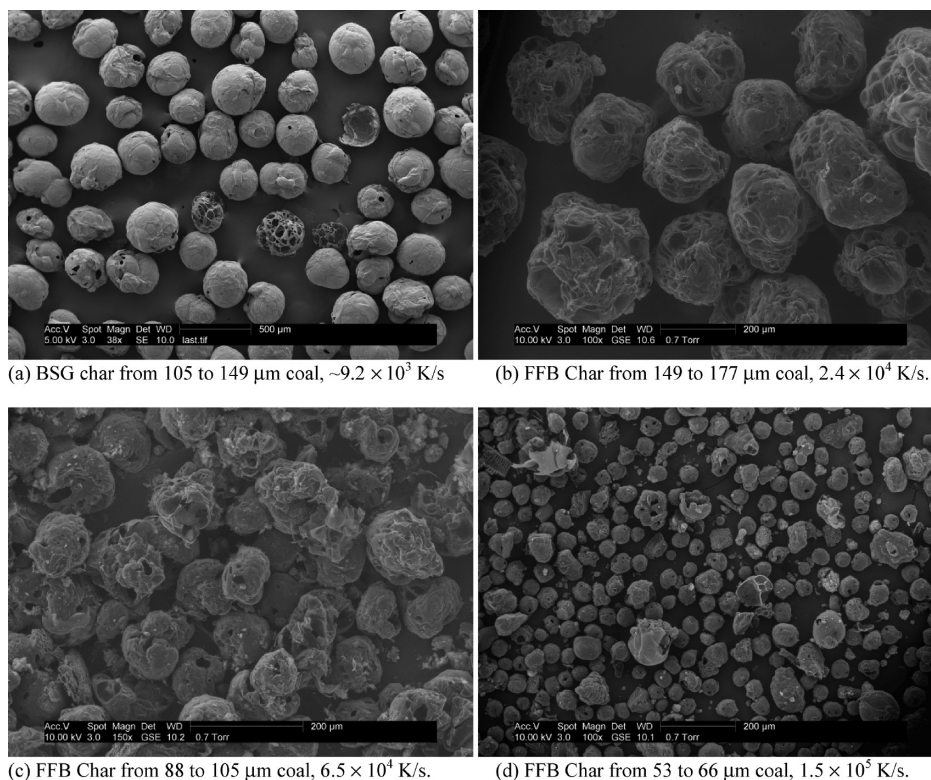


Figure 2. SEM images of eastern bituminous coal A chars produced at various heating rates (scales differ).

ash-free (daf) for all three coal sizes, as shown in Table 2. Al and Si elemental tracers were also used on the two larger size cuts, yielding volatiles of 67–70%.^{12,17} The ash tracer technique was used to determine mass release in the BSG; therefore, the ash tracer was also used for analysis of the FFB swelling results for consistency in the modeling work. The use of the ash tracer leads to swelling ratios 2–8% larger than those calculated using the more accurate Al and Si tracers.¹²

The tap technique was used to determine bulk densities of all coals and chars.^{4,5,18} The swelling ratio can be determined using the following relationship:

$$\frac{d}{d_0} = \left(\frac{\frac{m}{m_0}}{\frac{\rho}{\rho_0}} \right)^{1/3} = \left[\frac{\left(\frac{m}{m_0} \right)}{\left(\frac{\rho_b}{1 - \varepsilon_b} \right) \left(\frac{1 - \varepsilon_{b0}}{\rho_{b0}} \right)} \right]^{1/3} \quad (1)$$

where the terms with the subscript “0” refer to the parent coal and the other terms refer to the char. The residual mass ratio m/m_0 in this equation is expressed on an as-received basis. The density ratio ρ/ρ_0 refers to the ratio of apparent densities, where apparent density is defined as the mass of a particle divided by the total volume enclosed by the outer surface of the particle (assumed to be spherical). The bulk or bed density (ρ_b for the char and ρ_{b0} for the coal) is measured using the tap technique; it includes the volume in between particles.

The apparent density can be obtained from the bulk density using a packing factor or interparticle void fraction (ε_b for char and ε_{b0} for coal), which typically has a value of 0.45 for particles of nearly spherical geometry.^{5,18} In this work, the coal and the char particles were assumed to have approximately the same average shape and, hence, the same packing factor. With this assumption, the packing factors cancel out and the bulk densities can be used directly to determine the swelling ratio. The error associated with this method has been estimated to be 10%.¹⁸

When the experiments from the FFB and the BSG are plotted together, as in Figure 1, it becomes clear that swelling decreases rapidly at heating rates from slightly below 10^4 K/s until nearly 10^5 K/s. The consistency of the data from the two facilities is very good; there is no significant discontinuity in the trend. It appears that the swelling ratio has an asymptote of ~ 0.9 as the heating rate increases beyond 10^5 K/s. These new data confirm and clarify trends observed previously using a different facility and a different bituminous coal (Pittsburgh #8; Figure 1).⁵ The consistency of these results with the previous measurements implies that it is common for bituminous coals to exhibit large decreases in swelling at heating rates between 10^4 and 10^5 K/s. The effect of heating rate on swelling would be expected to be small for coals of very low or high ranks, but it is large for the steam coals that have been investigated thus far.

Scanning electron microscopy (SEM) images (Figures 2 and 3) of the FFB chars and a BSG char further illustrate the trends in swelling presented in Table 2. It is important to note the differences in scale in Figures 2 and 3, and remember that the largest char particles came from large coal particles. All chars were more spherical than the raw coal, which indicates that softening occurred at all of the heating rates investigated. It is apparent that, at lower heating rates, the chars are more cenospheric (hollow spheres) with much larger diameters, smoother surfaces, and thinner walls.

3. HIGH HEATING RATE MODEL DEVELOPMENT

Two major regimes of bituminous coal swelling behavior have been observed (Figure 1). Regime 2, corresponding to heating rates greater than $\sim 10^4$ K/s, is of primary interest for applications using pulverized coal. In this regime, swelling initially decreases rapidly with increasing heating rate up to $\sim 10^5$ K/s. It appears that the swelling ratio approaches an asymptotic minimum of ~ 0.9 at higher heating rates. This model is primarily

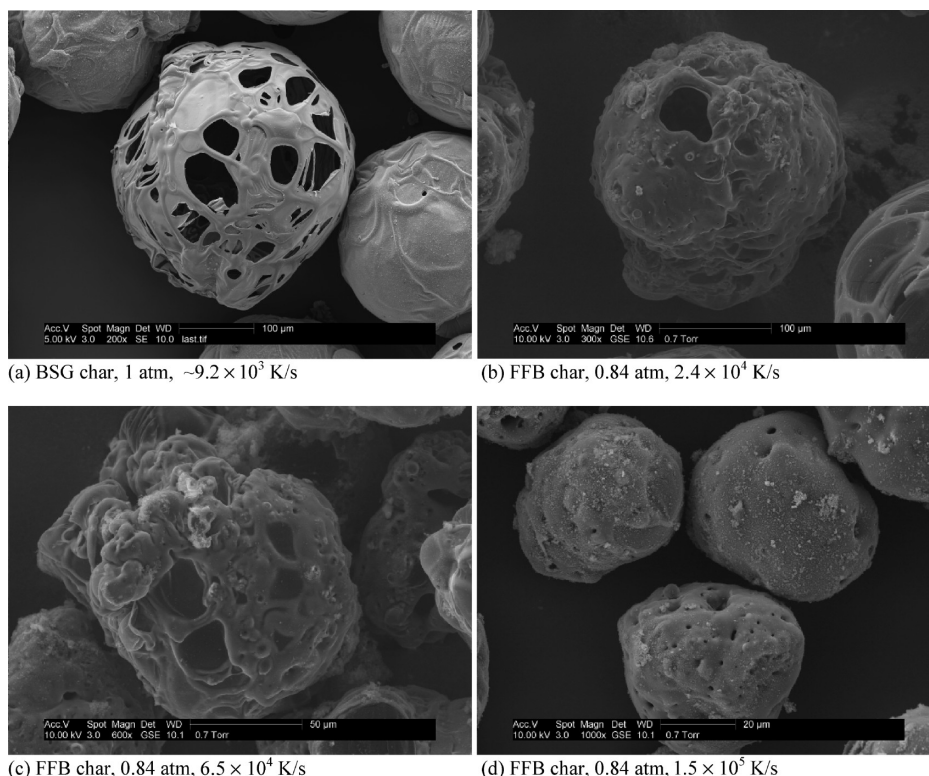


Figure 3. SEM images of eastern bituminous coal A char produced at 0.84 atm and various heating rates.

intended to represent behavior in regime 2. It is intended to represent coal swelling in dispersed entrained flow, primarily using laminar-flow experimental data. Fluid dynamics should not affect swelling, except through the heating rate, which is explicitly included in the model.

The heating rate that correlates best with swelling behavior is the maximum derivative of the particle temperature with respect to residence time, assuming lumped capacitance.

$$\dot{T} = \left(\frac{dT_p}{dt} \right)_{\max} \quad (2)$$

In a modeling study of drop-tube reactor conditions, calculated differences between the particle surface and center temperatures were small (<40 K) and the calculations agreed well with measured particle temperatures.¹⁹ The authors concluded that the lumped capacitance model was adequate for entrained-flow conditions with particles of $100 \mu\text{m}$ and heating rates of 10^4 K/s. The physical significance of the lumped-capacitance heating rate breaks down as the particle size and heating rate increase. Mass-transfer limitations also affect swelling for large particles.²⁰ This correlation is not recommended for particles larger than $\sim 200 \mu\text{m}$.

The heating rate was calculated using an energy balance that includes transient, convection, radiation, and reaction/vaporization terms.²¹ The energy balance was applied in a 1D model that uses the CPD code to describe pyrolysis.²² Correction factors have sometimes been used to reconcile calculated temperatures with optical measurements.²¹ Calculations that did not include a correction factor yielded modest errors in devolatilization times for particles with diameters near $50 \mu\text{m}$ but more significant errors for particles larger than $150 \mu\text{m}$. In this study, the correction factor was applied in the energy balance using the

Merrick heat capacity evaluated at 300 K.²³ This approach yielded calculated particle temperatures that were consistent with previous measurements and calculations.²¹ Further details of these calculations are documented elsewhere.¹²

The starting point for the development of the swelling correlation was a compilation of Sandia combustion and pyrolysis data.^{24,25} The wide range of coal ranks in the data set allows many of the effects of coal rank on swelling to be captured. The correlation matches observed shrinkage for lignites and sub-bituminous coals. Maximum swelling occurs at ranks slightly higher than high volatile A (hva) bituminous and describes decreasing swelling for even higher rank coals. The resulting model is simple enough for CFD applications and can be used as a guide for future experiments.

During model development, different coal properties and functional forms were tried to allow for a good fit of the Sandia bituminous coal data. A form of the swelling ratio that has the capability to match the observed swelling behavior at high heating rates (above $\sim 10^4$ K/s, denoted by subscript “HHR”) is

$$\left(\frac{d}{d_0} \right)_{\text{HHR}} = s_{\text{var}} \left(\frac{\dot{T}_{\text{base}}}{\dot{T}} \right)^{c_{\text{HR}}} + s_{\text{min}} \quad (3)$$

$$s_{\text{min}} = (\text{FC}_{\text{ASTM}} + A_{\text{ASTM}})^{1/3} \quad (4)$$

where FC_{ASTM} is the American Society for Testing and Materials (ASTM) fixed carbon and A_{ASTM} is the ASTM ash fraction on a dry basis. The parameter s_{min} represents the theoretical lower limit of swelling at infinitely high heating rates, assuming that the apparent particle density is constant and the trends in the volatiles yield with coal rank are well-represented by the ASTM volatiles. The parameter s_{var} can be determined from experimental data at an arbitrary

Table 3. Coal Properties for Correlation of s_{var} with Rank^{15,24}

coal	Beulah Zap	Lower Wilcox	Smith-Roland	Dietz	Blue #1
PSOC number	1507D	1443D	1520D	1488D	1445D
source state	North Dakota	Texas	Wyoming	Montana	New Mexico
rank	lignite A	lignite A	sub-bituminous C	sub-bituminous B	hVc bituminous
size (μm)	106–125	106–125	106–125	106–125	106–125
reactor, O ₂ (%)	CCL, 6% O ₂	CCL, 6% O ₂	CCL, 6% O ₂	CCL, 6% O ₂	CCL, 6% O ₂
collection height (mm)	64	64	64	64	64
C (% daf)	62.97	67.95	66.39	86.81	77.93
H (% daf)	4.42	5.33	5.22	5.81	5.49
N (% daf)	0.94	1.36	0.98	1.16	1.42
S (% daf)	2.00	1.36	1.76	0.40	0.71
O (% daf, by difference)	29.67	24.00	25.65	5.81	14.44
volatiles (% daf)	49.29	52.78	48.17	41.87	46.77
ash (% dry)	13.41	19.29	9.13	4.90	3.56
$(\sigma + 1)/M_\delta$	0.068	0.084	0.077	0.156	0.131
experimental d/d_0	0.92	0.93	0.87	1.07	1.16
heating rate (K/s)	6.07×10^4	5.93×10^4	6.19×10^4	5.34×10^4	5.90×10^4
free swelling index	0	0	0	0	0

coal	Hiawatha	Pittsburgh #8	Lower Kittanning	Pocahontas #3
PSOC number	1502D	1451D	1516D	1508D
source state	Utah	Pennsylvania	Pennsylvania	West Virginia
rank	hVc bituminous	hVa bituminous	lv bituminous	lv bituminous
size (μm)	106–125	106–125	106–125	106–125
reactor, O ₂ (%)	CCL, 6% O ₂	CCL, 6% O ₂	CCL, 6% O ₂	CCL, 6% O ₂
collection height (mm)	64	64	64	64
C (% daf)	79.69	82.62	82.76	89.01
H (% daf)	5.27	5.33	4.70	4.34
N (% daf)	1.22	1.77	1.41	1.03
S (% daf)	0.44	2.13	3.79	0.59
O (% daf, by difference)	13.38	8.14	7.34	5.03
volatiles (% daf)	37.24	39.83	21.18	17.18
ash (% dry)	7.17	9.95	28.48	17.04
$(\sigma + 1)/M_\delta$	0.143	0.164	0.208	0.246
experimental d/d_0	1.08	1.11	1.26	1.14
heating rate (K/s)	5.29×10^4	5.76×10^4	6.12×10^4	6.03×10^4
free swelling index	0.5	7.5	8.5	6.5

standard heating rate (denoted by the subscript “base”), where the heating rate ratio reduces to unity and the heating rate exponent c_{HR} can be ignored. The standard heating rate of 5.8×10^4 K/s was selected to correspond with the average of the heating rates calculated for the Sandia combustion data, which had a range from 5.3×10^4 to 6.1×10^4 K/s.

The CPD network devolatilization model makes use of chemical structural parameters that can be obtained from ¹³C nuclear magnetic resonance (NMR) spectroscopy.¹⁶ It seems logical that these same chemical structure properties would also affect coal swelling through the extent and rate of volatiles release and through their effect on viscoelastic properties of the pyrolyzing coal. Because NMR parameters are only available for a few coals, Genetti et al.¹⁵ developed correlations for these parameters based on the coal proximate and ultimate analyses. The chemical structure parameters used in the current swelling model were therefore obtained from Genetti's correlations, because the proximate and ultimate analyses are generally available.

The ratio $(\sigma + 1)/M_\delta$ was selected to correlate the s_{var} term from the Sandia combustion data (Table 3 and Figure 4). This ratio represents the average number of attachments per aromatic cluster $(\sigma + 1)$ divided by the average molecular weight of a side chain (M_δ). This ratio serves as a coal rank index; coals tend to have more cross-links, shorter chains, and less oxygen as rank and aromaticity increase. Some coals do not appear in their traditional rank orders when this index system is used, but the overall swelling trends made more sense using this system compared to other rank indices attempted, including combinations of other NMR parameters, elemental composition, and volatile matter. The ratio $(\sigma + 1)/M_\delta$ is closely related to the initial extent of cross-linking in the coal. At heating rates in regime 2, the characteristic relaxation time of the metaplast is longer than the characteristic time of devolatilization. Viscosity is very high for highly cross-linked polymers, which may explain why swelling correlates well with this index at these high heating rates. An

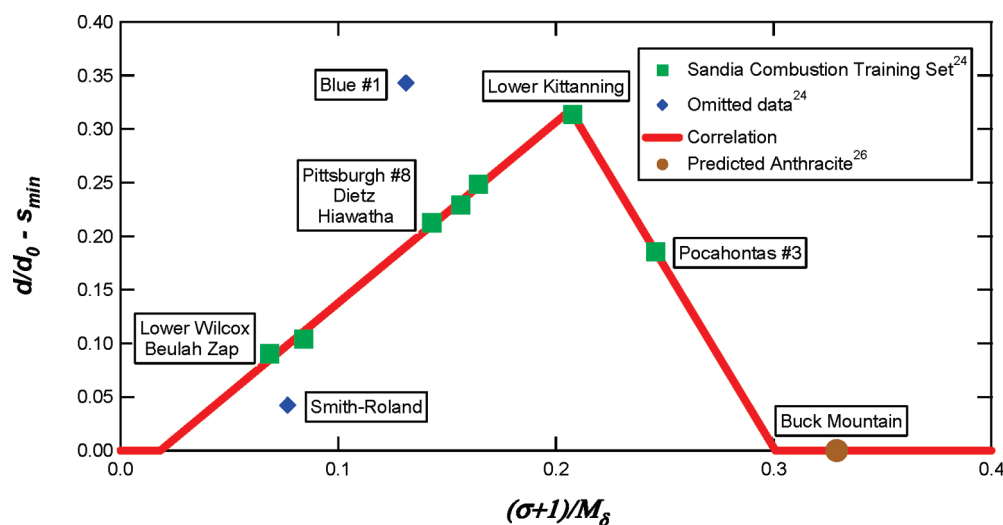


Figure 4. Correlation of s_{var} with NMR-based rank index using Sandia combustion data.^{24,26}

Table 4. Coal Properties for Correlation of c_{HR} with Rank

coal	Illinois #6	Blue #1	Pittsburgh #8	Pittsburgh #8	Pocahontas #3
PSOC number	1493D	1445D	1451D	1451D	1508D
source state	Illinois	New Mexico	Pennsylvania	Pennsylvania	West Virginia
rank	hvC bituminous	hvc bituminous	hva bituminous	hva bituminous	lv bituminous
size (μm)	106–125	106–125	106–125	63–75	106–125
reactor	CDL	CDL	CDL	CDL	CDL
collection height (mm)	250	250	250	250	250
C (% daf)	74.12	75.60	81.92	84.23	88.83
H (% daf)	4.96	5.26	6.45	5.54	4.37
N (% daf)	1.45	1.32	1.65	1.65	1.06
S (% daf)	6.29	0.49	1.26	1.01	0.60
O (% daf, by difference)	13.18	17.33	8.72	7.56	5.14
volatiles (% daf)	43.37	46.77	39.83	38.69	17.18
ash (% dry)	11.3	3.48	11.2	3.73	16.72
$(\sigma + 1)/M_\delta$	0.123	0.124	0.131	0.161	0.244
experimental d/d_0	1.13	1.12	1.31	1.37	1.22
heating rate (K/s)	1.69×10^4	1.95×10^4	1.38×10^4	2.66×10^4	1.49×10^4
free swelling index	3.0	0	7.5	7.5	6.5

index that is more closely related to aromaticity may be more appropriate for correlating swelling at heating rates in regime 1.

Data from two coals were omitted as non-representative (Blue #1 and Smith-Roland; Figure 4). This may indicate errors in the experimental data, errors in the calculated heating rate, limitations in the accuracy of the correlations for NMR parameters, or other limitations of the model. The presence of outliers is to be expected and indicates that other factors besides the properties in the selected rank index may be influential in swelling/shrinkage for some coals, especially under oxidizing conditions.

The free swelling index has traditionally been used as a qualitative measure of the swelling or caking characteristics of a coal, especially when large particles are used.²⁷ A comparison of the parameters in Table 3 and Figure 4 shows that the four non-zero free swelling indices have a trend that is somewhat consistent with the trends in the measured swelling ratios. However, the current model provides a more quantitative relationship between the coal

rank and the swelling ratio than the free swelling index, especially for small coal particles at high heating rates.

It seems reasonable that variations in the chemical structure with coal rank would cause the heating rate dependence of swelling (c_{HR}) to first increase and then decrease with increasing rank in a manner similar to s_{var} . Therefore, the same rank index was used for both s_{var} and c_{HR} . The heating rate exponent c_{HR} can be determined by rearranging eq 2, provided that s_{var} has already been determined for the coal of interest or pyrolysis swelling data are available at several heating rates. The parameter s_{var} is dependent upon the choice of the standard heating rate, but c_{HR} is independent of the standard heating rate.

Linear and quadratic fits of c_{HR} from the Sandia pyrolysis data set (see Table 4) are presented in Figure 5.²⁵ The piecewise linear fit assumes that maximum sensitivity to swelling occurs at the same rank index as maximum swelling and is shown to illustrate the ranks of high uncertainty. In the absence of more extensive

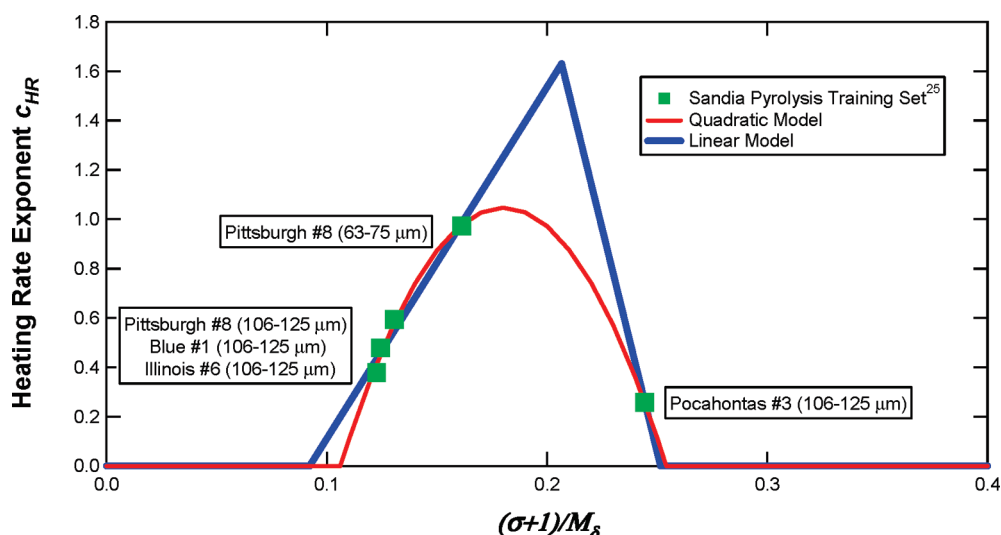


Figure 5. Heating rate exponent fitted to Sandia pyrolysis data.²⁵

Table 5. Correlations for s_{var} and c_{HR} with NMR-Based Rank Index $(\sigma + 1)/M_{\delta}$

correlation	range of applicability
$s_{\text{var}} = 1.69 \frac{\sigma + 1}{M_{\delta}} - 0.0309$	$0.018 \leq \frac{\sigma + 1}{M_{\delta}} < 0.207$
$s_{\text{var}} = -3.37 \frac{\sigma + 1}{M_{\delta}} + 1.01$	$0.207 \leq \frac{\sigma + 1}{M_{\delta}} \leq 0.301$
$s_{\text{var}} = 0$	$\frac{\sigma + 1}{M_{\delta}} < 0.018$ or $\frac{\sigma + 1}{M_{\delta}} > 0.301$
$c_{\text{HR}} = -191 \left(\frac{\sigma + 1}{M_{\delta}} \right)^2 + 68.9 \left(\frac{\sigma + 1}{M_{\delta}} \right) - 5.16$	$0.106 < \frac{\sigma + 1}{M_{\delta}} < 0.254$
$c_{\text{HR}} = 0$	$\frac{\sigma + 1}{M_{\delta}} < 0.106$ or $\frac{\sigma + 1}{M_{\delta}} > 0.254$

data, the quadratic fit is recommended because it yields more conservative estimates, especially for low-rank coals. The recommended correlations for s_{var} and c_{HR} are presented in Table 5. It is interesting to note that the value of c_{HR} calculated from the correlated value of s_{var} for Blue #1 coal fits the c_{HR} trend very well (Figure 5), even though this coal was omitted from the s_{var} correlation (Figure 4). This result suggests that the omission of the combustion measurement from the s_{var} correlation for this coal was justified.

4. COMPARISON TO ADDITIONAL DATA

Although much swelling data are available in the literature, such data are often unsuitable for comparison to this swelling model. The required ultimate and proximate analyses are usually provided, but there are exceptions.⁶ However, the heating rate is often not reported.²⁸ When the heating rate is reported, different definitions and/or calculation procedures are often used, rendering the heating rate unsuitable for use in this model.^{10,29} This model may yield very unrealistic swelling ratios if time-averaged particle heating rates are substituted for maximum instantaneous particle heating rates. Often only the order of magnitude is reported (or cited) for the heating rate, typically 10^4 K/s for a drop-tube reactor,³ which is insufficient to characterize swelling in the range from 10^4 to 10^5 K/s. The operating conditions are rarely reported in enough detail to allow for calculation of the particle temperature history. The heating rate is

somewhat sensitive to the moisture content of the coal; drying the coal before pyrolysis experiments at heating rates in regime 2 may enhance swelling.^{12,25}

Two data sets were used to evaluate the atmospheric swelling model, with each having a broad range of well-characterized heating rates (Figure 1). The first set was the eastern bituminous coal A data presented in this work, with a predicted rank index of 0.142. The second set consisted of data from Pittsburgh #8 coal in a drop-tube reactor, with a predicted rank index of 0.154.⁵ The quadratic fit of the heating rate exponent yielded very satisfactory results for both sets of bituminous coal data over the whole range of heating rates without further adjustment of model parameters. Only 2 calculated swelling ratios of 17 deviated from the corresponding experimental values by more than 0.1. This result is a significant improvement over previous attempts to fit the two data sets directly with a constant heating rate exponent.

The fit of the training and evaluation data sets at heating rates above $\sim 10^4$ K/s are presented in Figure 6. The CBK swelling correlation¹¹ is also shown for the Sandia combustion data (\square in Figure 6). The CBK swelling model (which lacks heating rate dependence) was developed from the same Sandia combustion data used to develop the current model.^{11,30,31} The current model yields a superior fit of the Sandia combustion data when compared to the CBK swelling correlation (Figure 6).

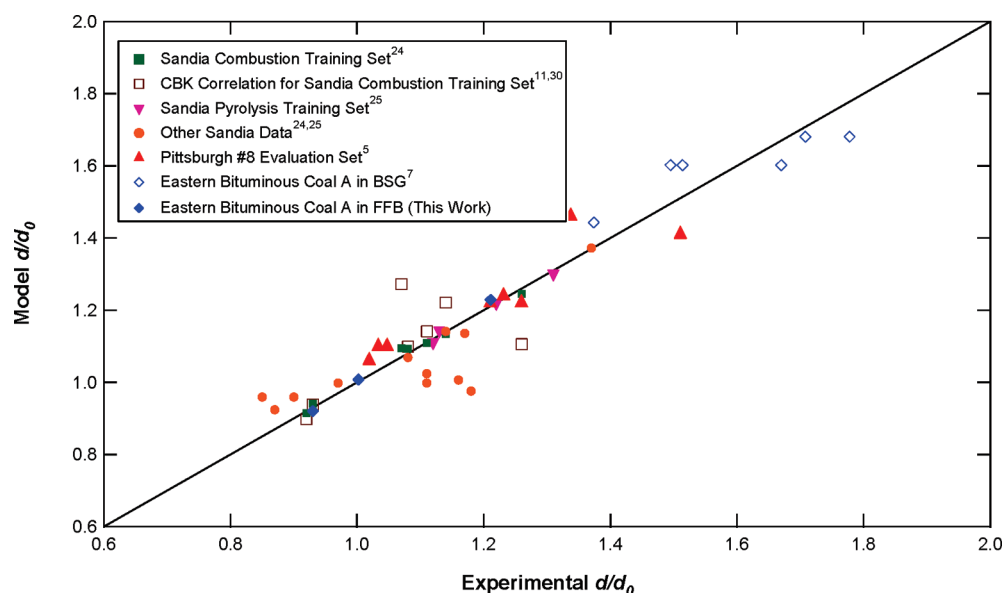


Figure 6. Swelling parity plot at heating rates above $\sim 10^4$ K/s.^{5,7,24,25} The CBK swelling model is also shown.¹¹

The other Sandia data presented in Figure 6 include eight coals that serve as a third data set to evaluate the swelling model. These data include combustion data from three coals of smaller size fractions (with higher heating rates) and also the two coals rejected from the s_{var} correlation (Figure 4).²⁴ Also included are data from seven Sandia pyrolysis experiments that were either from coals of smaller size fractions or conducted in a flat-flame burner rather than a drop-tube reactor.²⁵ The fit of the other Sandia data is generally excellent; all calculated swelling ratios deviated from the experimental values by less than 0.2, and only 4 of the 12 calculated swelling ratios deviated from experimental values by more than 0.1. Of those 4, 3 are Blue #1, which was omitted from the s_{var} correlation. The other coal with a higher deviation was Beulah Zap lignite under pyrolysis conditions. A total of 5 of the 12 calculated swelling ratios from the other Sandia data deviated from experimental values by 0.03 or less.

These three sets of data and the Sandia training sets include 11 types of coal with a wide range of ranks. Most of these coals were investigated at multiple heating rates using different particle sizes, experimental facilities, and operating conditions. Together, these data show that the effect of heating rate on coal swelling should not be ignored, especially for bituminous coals. The basic form of the swelling model as represented in eq 3 appears to be appropriate to represent effects of the heating rate and coal rank in regime 2. The approach of assigning most of the rank dependence to the s_{var} term appears to be robust, but some modest rank dependence in c_{HR} is required if the model is to be applied to coals from a wide range of ranks. The correlations for these two terms may need to be updated as appropriate data from more coals become available. However, the model in its current form appears to be an adequate foundation for the development of a more comprehensive model that includes the effects of pressure on swelling.

5. LOW HEATING RATE CORRELATION

For swelling at low heating rates (regime 1 of Figure 1), the data available were less suitable for direct regression of parameters. Thermogravimetric analyzers (TGAs) and wire mesh

reactors (WMRs) operate at heating rates from below 1 to 10^3 K/s and sometimes higher. Determination of swelling is difficult for these reactors because particles in a bed often fuse together and particles may also melt into the matrix of a heated grid.³² Experiments are often performed with coal particles larger than $200 \mu\text{m}$,^{6,33} where internal mass-transfer limitations begin to be influential.²⁰

Inspection of the heated grid data by Zygourakis⁶ shows that swelling in regime 1 increases approximately linearly with the logarithm of heating rate for Illinois #6 coal (Figure 1). Also, the swelling ratio at 1 K/s is greater than unity for this bituminous coal. The swelling ratio appears to be relatively constant below 1 K/s. However, in another heated grid study with $100 \mu\text{m}$ vitrinite particles, very few signs of plasticity were observed at 0.1 K/s.³² This contradicted trends observed in coking applications; the authors attributed the difference to the small, dispersed particles used in their study. It was proposed that, at 0.1 K/s, resistance to mass transfer in larger particles inhibits the release of tar, which plasticizes the coal melt and increases swelling.

The influence of heat- and mass-transfer limitations appears to have a complex dependence upon the heating rate. At higher heating rates, internal temperature gradients in large particles would cause material near the surface to generate volatiles faster than material near the center of the particle. Internal temperature gradients may also cause internal gradients in viscoelastic properties. The interplay between these and other transport effects could cause swelling to be enhanced or inhibited with increasing particle size, depending upon the details of particle size, coal type, and heating rate. Swelling data obtained from Pittsburgh #8 coal in a fixed bed at heating rates of 0.4 and 1.1 K/s indicated that the effects of pressure and heating rate on swelling can have very different trends for particles smaller than $75 \mu\text{m}$ compared to particles of $250\text{--}425 \mu\text{m}$.³⁴

The trends of the available experimental data were used in the current study to define a method to transfer the predicted composition dependence of the high heating rate model from regime 2 to regime 1.⁶ The approach chosen for the low heating rate (regime 1) model is very simple compared to the high heating rate (regime 2) model. The regime 1 correlation is presented mostly as a reminder

not to extrapolate the regime 2 model to heating rates much below 10^4 K/s. It is expected that the regime 2 model will be more useful for realistic pulverized coal applications.

Several assumptions are needed to use the trends of the Zygourakis data. First, it was assumed that all major transitions in swelling behavior happen near the same heating rates for all coals. Second, the heating rate corresponding to maximum swelling was assumed to be 8.5×10^3 K/s. This value of the heating rate was chosen to allow for coverage of the available regime 2 data without excessive extrapolation of the regime 2 model. This assumption can be adjusted when data become available to more precisely identify the location of peak swelling with respect to the heating rate or the magnitude of maximum swelling. Third, the Illinois #6 coal used by Zygourakis is assumed to have ultimate and proximate analyses similar to the corresponding Argonne premium coal sample, with only small transport limitations attributable to the large particles (250–300 μm). The form chosen for the low heating rate correlation is

$$\left(\frac{d}{d_0}\right)_{\text{LHR}} = m \log(\dot{T}) + b \quad (5)$$

Heating rates that yield regime 2 swelling ratios (eq 2) equivalent to those measured by Zygourakis in regime 1 were identified (Table 6 and Figure 7). The low heating rate model (eq 5) uses the composition dependence from the high heating rate model (eq 2) by transferring swelling ratios predicted in regime 2 to regime 1 and interpolating between them.

Table 6. Heating Rates in Regimes 1 and 2 with Equivalent Model Swelling Ratios

regime 1 heating rate (K/s)	regime 2 heating rate (K/s)
$\dot{T}_{\text{peak}} = 8.5 \times 10^3$	$\dot{T}_{\text{peak}} = 8.5 \times 10^3$
1000	$\dot{T}_{\text{mid}} = 1.63 \times 10^4$
1	$\dot{T}_{\text{low}} = 3.37 \times 10^4$

Figure 7 shows two piecewise methods to implement eq 5 for bituminous coals. A two-piece interpolation scheme yields no swelling at ~ 0.1 K/s and no major transitions in behavior from that point up to the regime change. A three-piece interpolation scheme provides a better fit of the Zygourakis data and features accelerated swelling above 10^3 K/s. Much more data in regime 1 would be needed to determine whether either of these methods will yield more accurate swelling ratios. For sub-bituminous coals and lignites, the use of eq 5 to interpolate between the maximum swelling ratio at 8.5×10^3 K/s and a swelling ratio of unity at 1 K/s should yield reasonable behavior. This approach yields reasonable regime 1 behavior (with the exception of the unrealistically sudden transitions in the slope of the swelling ratio versus heating rate) without requiring that additional parameters be fit to the insufficient data currently available.

6. DISCUSSION

In cases where the heating rate has been calculated properly and experimental swelling in regime 2 is not in good agreement with the model, the experimental data can be used to modify one or more terms of this correlation. Any deviations of calculated swelling ratios from measurements will be most pronounced at heating rates slightly below 10^4 K/s, near the transition between regimes 1 and 2. For some coals, fragmentation may be favored at the regime transition because of very thin cenosphere walls. Fragmentation reduces swelling ratios observed using either density measurements or image analysis.

A potential difficulty arises in implementing this swelling correlation into larger codes. The maximum particle heating rate must be calculated from an energy balance on the particle before the correlation can be used. A rigorous iterative solution technique would be computationally expensive, especially in a CFD subroutine. However, the maximum heating rate typically occurs before significant devolatilization has occurred.¹⁷ Therefore, it is not necessary to apply the swelling correlation until a maximum heating rate is found, which eliminates the need for iteration. A small initial peak in the heating rate typically occurs immediately

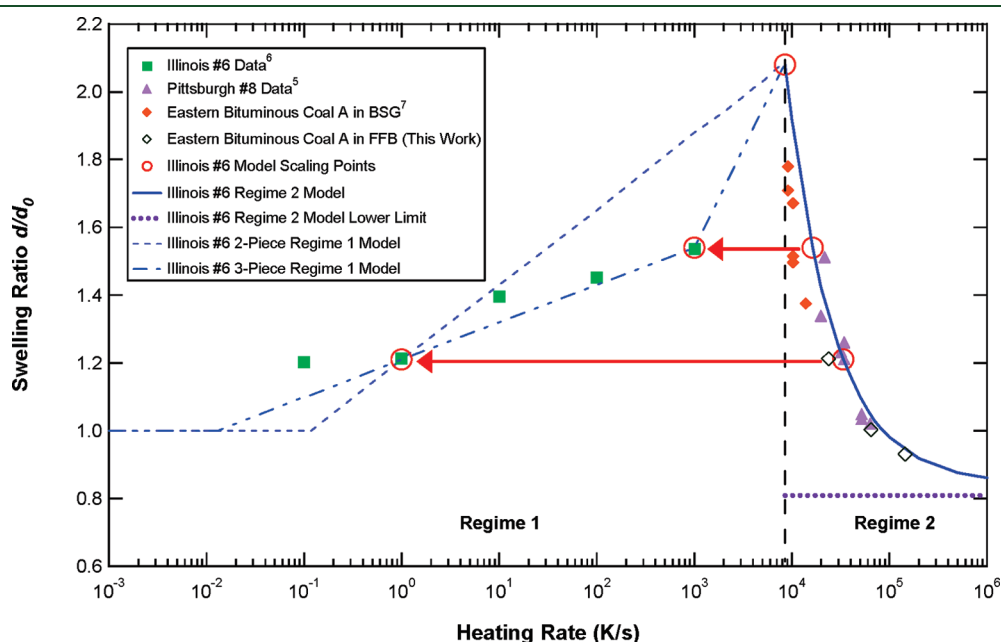


Figure 7. Complete swelling model (regimes 1 and 2) for Illinois #6 data by Zygourakis.^{5–7}

before water begins to vaporize, followed by a true maximum heating rate after water vaporization is complete.^{12,17} The moisture content should be checked at the time corresponding to each local maximum in heating rate to ensure that the correct heating rate is used for this swelling model.

As a low-cost alternative, an order-of-magnitude estimate for the heating rate may be assumed on the basis of the experimental or industrial device being modeled. Because of the asymptotic behavior of the swelling correlation, a utility boiler heating rate of 10^6 K/s may be used to calculate swelling ratios with very small error attributable to the uncertainty in the heating rate. An order-of-magnitude estimate of 10^4 K/s for a conventional drop-tube reactor may produce large errors in the calculated swelling ratio for bituminous coals because of the high sensitivity of the model to heating rate at this order of magnitude.

In real systems, swelling does not occur instantly. A common modeling approach is to apply the swelling or shrinkage in a linear fashion proportional to the release of volatiles.³⁵ Other measures of the extent of pyrolysis could be used, such as the fraction of metaplast or the extent of cross-linking. This approach is sufficient for most models of utility boilers because swelling is low and devolatilization is fast at $\sim 10^6$ K/s.

If sufficient transient swelling data are available, then a new relationship could be devised to relate transient swelling to the extent of pyrolysis. Measurements of partially pyrolyzed coals indicate that the transient swelling ratio may exceed the final swelling ratio by 3–20%.²⁵ This can be explained in terms of bubbles collapsing as they burst, before cross-linking has advanced sufficiently to cause the metaplast to stiffen. The current model is only intended to estimate the swelling ratio of the fully pyrolyzed char.

7. CONCLUSION

Coal pyrolysis experiments with eastern bituminous coal A at atmospheric pressure and heating rates of 10^4 – 10^5 K/s confirmed the strong dependence of swelling upon heating rate observed previously for Pittsburgh #8. It appears that maximum swelling occurs for bituminous coals at heating rates slightly less than 10^4 K/s. Swelling seems to approach an asymptotic minimum with a value of d/d_0 slightly less than 1.0 as the particle heating rate increases above 10^5 K/s.

A correlation for coal swelling during atmospheric pyrolysis suitable for CFD applications was developed. The form of the model allows for the observed swelling trends to be correctly calculated. Model parameters were correlated with literature data using a rank index based on NMR structural parameters. This correlation was used to accurately predict swelling during pyrolysis at atmospheric pressure for eastern bituminous coal A and Pittsburgh #8 bituminous coals at several heating rates in the range of 10^4 – 10^5 K/s. A comparison of the model to additional swelling data from coals that were used in the model training set also shows that the model is capable of predicting differences in swelling with varying heating rate. This implies that the basic form of the model is robust and appropriate for modeling coal swelling at heating rates greater than $\sim 10^4$ K/s. A form has also been proposed to extrapolate the composition dependence of the high heating rate model to heating rates below 10^4 K/s while maintaining expected trends.

AUTHOR INFORMATION

Corresponding Author

*E-mail: tom_fletcher@byu.edu.

ACKNOWLEDGMENT

Thanks are due to Dr. Boris Eiteneer (deceased) and his co-workers at GE Global Research for their collaborative role in the study of the effect of heating rate on swelling. John Sowa at BYU provided valuable assistance and discussions, contributing to the development of a more consistent method to calculate particle temperature histories. This material is based on work supported by the Department of Energy under Award DE-NT0005015.

NOMENCLATURE

A = ash fraction (from ASTM proximate analysis, dry basis)
 b = logarithmic intercept in low heating rate swelling correlation
 BSG = bench-scale gasifier
 c_{HR} = coefficient in swelling correlation relating to heating rate
 d = diameter (m)
 d/d_0 = swelling ratio
 FC = fixed carbon fraction (from ASTM proximate analysis, dry basis)
 FFB = flat-flame burner
 m = mass (kg), logarithmic slope in low heating rate swelling correlation
 M_δ = mass per side chain (from ^{13}C NMR data)
 s_{var} = coefficient in swelling correlation relating to the coal structure
 s_{min} = coefficient in swelling correlation relating to the minimum size
 t = time (s)
 T = temperature (K)
 \dot{T} = heating rate (K/s)
 TGA = thermogravimetric analyzer
 VM = volatile matter fraction (from ASTM proximate analysis, dry and ash-free basis)
 WMR = wire mesh reactor
 ε = packing factor
 ρ = density (kg/m^3)
 $\sigma + 1$ = coordination number (attachments per cluster) from ^{13}C NMR data

Subscripts

ASTM = from ASTM proximate analysis
 b = bulk or bed
 base = baseline condition
 HHR = high heating rate ($>8.5 \times 10^3$ K/s)
 LHR = low heating rate ($<8.5 \times 10^3$ K/s)
 low = low value
 mid = mid-range value
 min = minimum
 max = maximum
 peak = peak value
 p = particle
 0 = initial

REFERENCES

- (1) Smoot, L. D.; Smith, P. J. *Coal Combustion and Gasification*; Plenum Press: New York, 1985; p 443.
- (2) Yu, J.; Lucas, J. A.; Wall, T. F. Formation of the structure of chars during devolatilization of pulverized coal and its thermoproperties: A review. *Prog. Energy Combust. Sci.* **2007**, 33 (2), 135–170.
- (3) Lee, C. W.; Scaroni, A. W.; Jenkins, R. G. Effect of pressure on the devolatilization and swelling behavior of a softening coal during rapid heating. *Fuel* **1991**, 70 (8), 957–965.

- (4) Fletcher, T. H. Swelling properties of coal chars during rapid pyrolysis and combustion. *Fuel* **1993**, 72 (11), 1485–1495.
- (5) Gale, T. K.; Bartholomew, C. H.; Fletcher, T. H. Decreases in the swelling and porosity of bituminous coals during devolatilization at high heating rates. *Combust. Flame* **1995**, 100 (1–2), 94–100.
- (6) Zygourakis, K. Effect of pyrolysis conditions on the macropore structure of coal-derived chars. *Energy Fuels* **1993**, 7 (1), 33–41.
- (7) Eiteneer, B.; Subramanian, R.; Maghzi, S.; Zeng, C.; Guo, X.; Long, Y.; Chen, L.; JS, R.; Raman, A.; Jain, J.; Fletcher, T.; Shurtz, R. Gasification kinetics: Modeling tools development and validation. *Proceedings of the 26th Annual International Pittsburgh Coal Conference*; Pittsburgh, PA, Sept 20–23, 2009.
- (8) Oh, M. S.; Peters, W. A.; Howard, J. B. An experimental and modeling study of softening coal pyrolysis. *AIChE J.* **1989**, 35 (5), 775–792.
- (9) Yu, J.; Lucas, J.; Wall, T.; Liu, G.; Sheng, C. Modeling the development of char structure during the rapid heating of pulverized coal. *Combust. Flame* **2004**, 136 (4), 519–532.
- (10) Kiden, K.; Yamashita, T.; Akimoto, A. Prediction of thermal swelling behavior on rapid heating using basic analytical data. *Energy Fuels* **2007**, 21 (2), 1038–1041.
- (11) Niksa, S.; Liu, G. S.; Hurt, R. H. Coal conversion submodels for design applications at elevated pressures. Part I. devolatilization and char oxidation. *Prog. Energy Combust. Sci.* **2003**, 29 (5), 425–477.
- (12) Shurtz, R. C. Effects of pressure on the properties of coal char and soot under gasification conditions at high initial heating rates. Ph.D. Dissertation, Department of Chemical Engineering, Brigham Young University, Provo, UT, 2011 (in progress).
- (13) Ma, J.; Fletcher, T. H.; Webb, B. W. Conversion of coal tar to soot during coal pyrolysis in a post-flame environment. *Symp. (Int.) Combust., [Proc.]* **1996**, 26 (2), 3161–3167.
- (14) Zhang, H.; Fletcher, T. H. Nitrogen transformations during secondary coal pyrolysis. *Energy Fuels* **2001**, 15, 1512–1522.
- (15) Genetti, D.; Fletcher, T. H.; Pugmire, R. J. Development and application of a correlation of ^{13}C NMR chemical structural analyses of coal based on elemental composition and volatile matter content. *Energy Fuels* **1999**, 13 (1), 60–68.
- (16) Fletcher, T. H.; Kerstein, A. R.; Pugmire, R. J.; Solum, M. S.; Grant, D. M. Chemical percolation model for devolatilization. 3. Direct use of carbon-13 NMR data to predict effects of coal type. *Energy Fuels* **1992**, 6 (4), 414–431.
- (17) Fletcher, T. H. Time-resolved particle temperature and mass loss measurements of a bituminous coal during devolatilization. *Combust. Flame* **1989**, 78 (2), 223–236.
- (18) Tsai, C.-Y.; Scaroni, A. W. The structural changes of bituminous coal particles during the initial stages of pulverized-coal combustion. *Fuel* **1987**, 66, 200–206.
- (19) Hardesty, D. R.; Fletcher, T. H.; Mitchell, R. E.; Baxter, L. L. *Coal Combustion Science Quarterly Progress Report January–March 1990*; Sandia National Laboratory: Livermore, CA, 1990.
- (20) Solomon, P. R.; Fletcher, T. H. Impact of coal pyrolysis on combustion. *Symp. (Int.) Combust., [Proc.]* **1994**, 25, 463–474.
- (21) Fletcher, T. H. Time-resolved temperature measurements of individual coal particles during devolatilization. *Combust. Sci. Technol.* **1989**, 63 (1–3), 89–105.
- (22) Fletcher, T. H. CPDCP_NLG code, http://www.et.byu.edu/~tom/cpd/cpdcpnlg/cpdcp_nlgfiles.html.
- (23) Maloney, D. J.; Sampath, R.; Zondlo, J. W. Heat capacity and thermal conductivity considerations for coal particles during early stages of rapid heating. *Combust. Flame* **1999**, 116, 94–104.
- (24) Mitchell, R. E.; Hurt, R. H.; Baxter, L. L.; Hardesty, D. R. *Compilation of Sandia Coal Char Combustion Data and Kinetic Analyses. Milestone Report*; Sandia National Laboratory: Livermore, CA, 1992; p 615.
- (25) Fletcher, T. H.; Hardesty, D. R. *Compilation of Sandia Coal Devolatilization Data: Milestone Report*; Sandia National Laboratory: Livermore, CA, 1992; p 346.
- (26) Smith, K. L.; Smoot, L. D.; Fletcher, T. H.; Pugmire, R. J. *The Structure and Reaction Processes of Coal*; Plenum Press: New York, 1994; p 471.
- (27) Speight, J. G. *Handbook of Coal Analysis*; Wiley: New York, 2005; p 240.
- (28) Feroso, J.; Gil, M. V.; Borrego, A. G.; Pevida, C.; Pis, J. J.; Rubiera, F. Effect of the pressure and temperature of devolatilization on the morphology and steam gasification reactivity of coal chars. *Energy Fuels* **2010**, 24, 5586–5595.
- (29) Yoshizawa, N.; Maruyama, K.; Yamashita, T.; Akimoto, A. Dependence of microscopic structure and swelling property of DTF chars upon heat-treatment temperature. *Fuel* **2006**, 85 (14–15), 2064–2070.
- (30) Hurt, R.; Sun, J.-K.; Lunden, M. A kinetic model of carbon burnout in pulverized coal combustion. *Combust. Flame* **1998**, 113 (1–2), 181–197.
- (31) Hurt, R. H. Personal communication regarding details of CBK codes; Shurtz, R., Ed.; 2010.
- (32) Hamilton, L. H. A preliminary account of char structures produced from Liddell vitrinite pyrolysed at various heating rates. *Fuel* **1980**, 59 (2), 112–116.
- (33) Khan, M. R.; Jenkins, R. G. Swelling and plastic properties of coal devolatilized at elevated pressures: An examination of the influences of coal type. *Fuel* **1986**, 65 (5), 725–731.
- (34) Khan, M. R.; Jenkins, R. G. Thermoplastic properties of coal at elevated pressures: 1. Evaluation of a high-pressure microdilometer. *Fuel* **1984**, 63 (1), 109–115.
- (35) Smoot, L. D.; Pratt, D. T. *Pulverized Coal Combustion and Gasification*; Plenum Press: New York, 1979.

NOTE ADDED AFTER ASAP PUBLICATION

The caption of Figure 4 was incorrect in the version of this paper published April 27, 2011. The correct version published May 4, 2011.